Universität Stuttgart

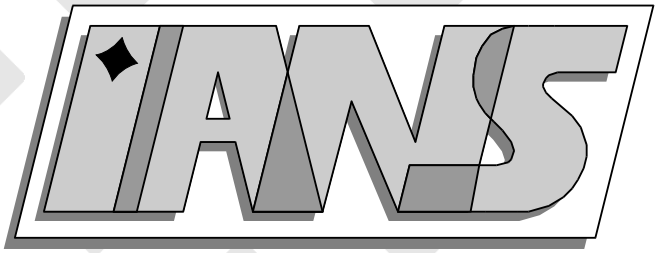

Stable Lagrange multipliers for quadrilateral meshes of curved interfaces in 3D

Bernd Flemisch, Barbara Wohlmuth

Berichte aus dem Institut für Angewandte Analysis und Numerische Simulation

Preprint 2005/005

Universität Stuttgart

Stable Lagrange multipliers for quadrilateral meshes of curved interfaces in 3D

Bernd Flemisch, Barbara Wohlmuth

Berichte aus dem Institut für Angewandte Analysis und Numerische Simulation

Preprint 2005/005

Institut für Angewandte Analysis und Numerische Simulation (IANS)
Fakultät Mathematik und Physik
Fachbereich Mathematik
Pfaffenwaldring 57
D-70 569 Stuttgart

E-Mail: ians-preprints@mathematik.uni-stuttgart.de
WWW: http://preprints.ians.uni-stuttgart.de

ISSN **1611-4176**

STABLE LAGRANGE MULTIPLIERS FOR QUADRILATERAL MESHES OF CURVED INTERFACES IN 3D

BERND FLEMISCH AND BARBARA I. WOHLMUTH

Abstract. The lowest order dual Lagrange multipliers are extended to arbitrary quadrilateral or triangular surface grids. In a first step, two alternatives are provided for the case of planar interfaces. For the approximation of vector fields, two more modifications are given for use on curvilinear interfaces. A priori results are obtained and several numerical examples are shown.

1. Introduction

When domain decomposition techniques are applied to discretize partial differential equations, it is always convenient and sometimes even mandatory to be able to deal with non-matching grids. There are numerous tasks where non-matching grids naturally arise when employing on each subdomain the grid which is best suited to solve the corresponding subproblem associated with this subdomain. The framework of mortar finite elements, [2, 3, 4, 15, 16], provides a method which is able to deal with non-matching grids both from the mathematical and from the implementational point of view. The method is based on introducing additional degrees of freedom in form of Lagrange multipliers on the interface. The numerical efficiency of the method can be considerably increased by using dual basis functions for the discrete Lagrange multiplier space, [17]. For quadrilateral surface grids, these basis functions have only been developed for parallelograms. In this paper, we extend the lowest order dual Lagrange multipliers to arbitrary quadrilateral or triangular surface grids. These surface grids may be discretizations of a possibly curvilinear interface.

The rest of this paper is outlined as follows. In Section 2, the abstract weak continuous and discrete problem formulations are introduced, and the advantages of using dual Lagrange multipliers are recalled. Section 3 contains a short account of the model problems which we intend to solve. Afterwards, we introduce lowest order dual Lagrange multiplier spaces for general quadrilaterals in Section 4. There, we focus on planar interfaces and scalar model equations. In principle, the extension to curvilinear interfaces is straightforward and covered by the theory. However, for the transmission of vectorial quantities, we encounter in some cases a preasymptotic misbehavior in form of unphysical oscillations along the interface. Therefore, Section 5 is devoted to present modifications to cure this misbehavior while preserving the advantages of the dual approach. Finally, we present an application in form of a nonlinear elasticity problem in Section 6.

2. Motivation

In the following, we illustrate why dual Lagrange multipliers are an important key to efficiently solve problems discretized by mortar finite elements. For the ease of notation and to avoid technicalities, we restrict ourselves to the case of two non-overlapping open subdomains Ω^{m} and Ω^{s} sharing a common interface Γ, their union giving the global domain Ω, $\overline{\Omega} = \overline{\Omega^{\mathrm{m}} \cup \Omega^{\mathrm{s}}}$. By taking into account the standard modifications at the cross-points or at the wire-basket of more than two subdomains, the following considerations apply analogously to decompositions into many subdomains, [3]. We focus on saddle point problems of the following structure, [2]: find a primal variable

SUPPORTED BY THE DEUTSCHE FORSCHUNGSGEMEINSCHAFT, SFB 404, TP B8, C12.

$u = (u^{\mathrm{m}}, u^{\mathrm{s}}) \in X = X^{\mathrm{m}} \times X^{\mathrm{s}}$ and a Lagrange multiplier $\lambda \in M$ such that

$$a(u, v) + b(v, \lambda) = f(v), \qquad v \in X, \tag{1a}$$

$$b(u, \mu) \qquad\quad = 0, \qquad\quad \mu \in M, \tag{1b}$$

with a bilinear form $a(\cdot,\cdot) = \sum_{k=\mathrm{m,s}} a_k(\cdot,\cdot)$ and a coupling bilinear form

$$b(v, \mu) = \langle [v], \mu \rangle_{M' \times M}, \tag{2}$$

where $[v] = v^{\mathrm{s}} - v^{\mathrm{m}}$ denotes the jump across the interface Γ, and $\langle \cdot, \cdot \rangle_{M' \times M}$ stands for the duality pairing on $M' \times M$. We assume that $a(\cdot,\cdot)$ is elliptic on the constrained space

$$V = \{ v \in X : b(v, \mu) = 0,\ \mu \in M \},$$

where in case of the Laplace operator, [10], and of the linear elasticity setting, [11], it is well known that the ellipticity constant does not depend on the number of subdomains. The saddle point problem (1) can be equivalently reformulated as the positive definite problem of finding $u \in V$ such that

$$a(u, v) = f(v), \qquad v \in V. \tag{3}$$

The approximation of X and M by finite element spaces $X_h = X_h^{\mathrm{m}} \times X_h^{\mathrm{s}}$ and M_h is based on two triangulations $\mathcal{T}_{\mathrm{m}}$ of Ω^{m} and $\mathcal{T}_{\mathrm{s}}$ of Ω^{s}. Using superscripts, we indicate by $\mathcal{T}^{\mathrm{m}}$ and $\mathcal{T}^{\mathrm{s}}$ the corresponding surface grids meeting the interface Γ. The finite element nodes on $\mathcal{T}^{\mathrm{m}}$ and $\mathcal{T}^{\mathrm{s}}$ are called master and slave nodes, respectively, all remaining nodes are indicated as inner nodes. The discrete Lagrange multiplier space M_h is associated with the mesh $\mathcal{T}^{\mathrm{s}}$ on the slave side. The corresponding discretization of problem (1) can be written as

$$\begin{pmatrix} A_{\mathrm{ii}} & A_{\mathrm{im}} & A_{\mathrm{is}} & 0 \\ A_{\mathrm{mi}} & A_{\mathrm{mm}} & 0 & -M^{\mathrm{T}} \\ A_{\mathrm{si}} & 0 & A_{\mathrm{ss}} & D^{\mathrm{T}} \\ 0 & -M & D & 0 \end{pmatrix} \begin{pmatrix} u_h^{\mathrm{i}} \\ u_h^{\mathrm{m}} \\ u_h^{\mathrm{s}} \\ \lambda_h \end{pmatrix} = \begin{pmatrix} f^{\mathrm{i}} \\ f^{\mathrm{m}} \\ f^{\mathrm{s}} \\ 0 \end{pmatrix}, \tag{4}$$

where the subscripts i, m, and s represent the inner, master and slave nodes, respectively. The entries of the coupling matrices M and D are assembled from integrals of the form

$$\int_\Gamma \phi_p^{\mathrm{m}} \mu_q \, \mathrm{d}\Gamma, \quad \text{and} \quad \int_\Gamma \phi_p^{\mathrm{s}} \mu_q \, \mathrm{d}\Gamma,$$

respectively, where ϕ_p^k, $k = \mathrm{m}, \mathrm{s}$, denotes the scalar nodal basis function of the trace space $W_h^k = X_h^k|_\Gamma$ of the finite element space on $\mathcal{T}^k$ associated with the node p, and μ_q stands for the scalar basis function of the discrete Lagrange multiplier space M_h associated with the node q. We speak of *dual* basis functions μ_q, if they satisfy the biorthogonality relation

$$\int_\Gamma \phi_p^{\mathrm{s}} \mu_q \, \mathrm{d}\Gamma = \delta_{pq} \int_\Gamma \phi_p^{\mathrm{s}} \, \mathrm{d}\Gamma. \tag{5}$$

The importance of (5) comes into play when attempting to solve the discrete problem (4). There exist various possibilities for solving the problem efficiently by iterative solvers. The development of positive definite discrete formulations, which are equivalent to (4) and for which multigrid schemes can be applied, always involves the elimination of the discrete Lagrange multipliers from the indefinite system (4), [18]. This elimination is performed in terms of the discrete projection operator $\widehat{M} = D^{-1} M$, which enters into the positive definite system matrix. The same operator plays an essential role if Dirichlet–Neumann solvers are applied, [12, 13]. Depending on the structure of D, this projection can be carried out locally or it has to be carried out globally, represented by a sparse or a dense matrix $\widehat{M}$, respectively. In particular, if the biorthogonality relation (5) is satisfied, the matrix D is diagonal, and therefore, $\widehat{M}$ is sparse and can be easily calculated. We emphasize that the applicability of dual Lagrange multipliers is not restricted to linear stationary problems as (1). In more general cases, one has to face a linear system of the structure (4) in each iteration step of a time integration and/or nonlinear solution method. For example, the advantages of the dual approach have been fully exploited for the solution of contact problems, [14]. There, the linearized non-penetration condition is formulated as a weak

integral inequality constraint $Du_h^{\mathrm{s}} \leq Mu_h^{\mathrm{m}} + g^{\mathrm{s}}$. Only in case of dual Lagrange multipliers, this is equivalent to the point-wise inequality $u_h^{\mathrm{s}} \leq D^{-1}(Mu_h^{\mathrm{m}} + g^{\mathrm{s}})$.

3. Model problems

We introduce the model equations underlying the saddle point problem (1), which we use for our numerical illustrations. For scalar problems, we focus on Poisson's equation in $\mathbb{R}^3$. In particular, we seek a scalar function u as the solution of

$$-\Delta u = f \text{ in } \Omega, \tag{6}$$

with appropriate boundary conditions on $\partial\Omega$. The Lagrange multiplier λ is chosen to be the normal flux through the interface Γ, i.e., $\lambda = -\partial u/\partial \boldsymbol{n}$, with $\boldsymbol{n}$ denoting the unit outward normal vector field with respect to Ω^{s}. The spaces X^{s} and X^{m} are subsets of $H^1(\Omega^{\mathrm{s}})$ and $H^1(\Omega^{\mathrm{m}})$, respectively, such that given Dirichlet conditions on the boundary of the global domain Ω are respected. The product space $X = X^{\mathrm{m}} \times X^{\mathrm{s}}$ is equipped with the broken H^1-norm. The Lagrange multiplier space M is associated with the dual of the trace space of X^{s} on Γ, equipped with the dual norm.

Additionally, we consider linear and nonlinear elasticity problems. For the linear setting, we intend to solve (1) with spaces and (bi-)linear forms given by the weak form of the linear elasticity problem of finding a displacement vector field $\boldsymbol{u}$ such that

$$-\mathrm{div}\,\sigma(\boldsymbol{u}) = f \text{ in } \Omega, \tag{7}$$

supplemented by boundary conditions, by the Saint-Venant Kirchhoff law

$$\sigma = \lambda_{\mathrm{L}}(\mathrm{tr}\,\varepsilon)\mathrm{Id} + 2\mu_{\mathrm{L}}\,\varepsilon, \tag{8}$$

with the Lamé constants $\lambda_{\mathrm{L}}, \mu_{\mathrm{L}}$ and by the linearized strain tensor

$$\varepsilon(\boldsymbol{u}) = \frac{1}{2}(\nabla\boldsymbol{u} + [\nabla\boldsymbol{u}]^{\mathrm{T}}) \ . \tag{9}$$

Here, the Lagrange multiplier λ corresponds to the surface tractions on Γ, namely, $\lambda = -\sigma(\boldsymbol{u})\boldsymbol{n}$. The spaces X and M consist of vector fields with component functions being in the corresponding spaces for the scalar case.

However, the validity of the linearized elasticity equations (7)-(9) is restricted to small strains and small deformations. If the strains remain small but the deformations become large, one has at least to consider the geometrically nonlinear elasticity setting. This amounts to using the full Green–St. Venant tensor

$$E = \frac{1}{2}(F^{\mathrm{T}}F - \mathrm{Id}) = \frac{1}{2}(C - \mathrm{Id}), \tag{10}$$

instead of (9), with $F = \mathrm{Id} + \nabla\boldsymbol{u}$ the deformation gradient and $C = F^{\mathrm{T}}F$ the right Cauchy–Green strain tensor. We keep the constitutive law (8) as

$$S = \lambda_{\mathrm{L}}(\mathrm{tr}\,E)\mathrm{Id} + 2\mu_{\mathrm{L}}\,E = \mathcal{C}E, \tag{11}$$

defining the second Piola–Kirchhoff stress tensor S, with $\mathcal{C}$ the Hooke-tensor. We solve

$$-\mathrm{div}\,(FS) = f, \tag{12}$$

complemented by appropriate boundary conditions. In the weak setting, this yields the linear form $a(\boldsymbol{u}, \cdot)$ given by $a(\boldsymbol{u}, \boldsymbol{v}) = \sum_{i=1}^{4} a_i(\boldsymbol{u}, \boldsymbol{v})$, where

$$\begin{aligned} a_1(\boldsymbol{u}, \boldsymbol{v}) &= \int_\Omega \mathcal{C}\varepsilon(\boldsymbol{u}) : \varepsilon(\boldsymbol{v})\,dx, & a_2(\boldsymbol{u}, \boldsymbol{v}) &= \frac{1}{2}\int_\Omega \mathcal{C}\left[(\nabla\boldsymbol{u})^\top\nabla\boldsymbol{u}\right] : \nabla\boldsymbol{v}\,dx, \\ a_3(\boldsymbol{u}, \boldsymbol{v}) &= \int_\Omega \nabla\boldsymbol{u}\,\mathcal{C}\,\nabla\boldsymbol{u} : \nabla\boldsymbol{v}\,dx, & a_4(\boldsymbol{u}, \boldsymbol{v}) &= \frac{1}{2}\int_\Omega \nabla\boldsymbol{u}\,\mathcal{C}\left[(\nabla\boldsymbol{u})^\top\nabla\boldsymbol{u}\right] : \nabla\boldsymbol{v}\,dx. \end{aligned}$$

Still, the applicability of (10)–(12) is limited to small strains. In order to extend the model to large strains, we have to introduce another kind of nonlinearity by means of nonlinear material laws. In particular, to solve (12), we employ the Neo–Hooke law given by

$$S = \mu_{\mathrm{L}}(\mathrm{Id} - C^{-1}) + \frac{\lambda_{\mathrm{L}}}{2}(J^2 - 1)C^{-1}, \tag{13}$$

with $J = \det(F)$ denoting the determinant of the deformation gradient. While in (10) the nonlinearity enters in terms of polynomials of $\nabla \boldsymbol{u}$, it is given in terms of its inverse in (13).

Despite the complexity of the nonlinear setting, the subdomain coupling via Lagrange multipliers remains the same as for linear problems. In order to calculate a numerical solution, we eliminate the discrete Lagrange multipliers and apply a Newton iteration to the constrained problem. We note that this elimination is very efficient when we use the dual basis functions for spanning the Lagrange multiplier space. Moreover, the Jacobian of the constrained system is positive definite and admits the use of multigrid solvers for the linear system in each Newton step. Although dual Lagrange multipliers are quite attractive from the point of view of efficient solvers, they are more sensitive than standard Lagrange multipliers with respect to the element shape. In the following two sections, we address the local construction in case of general quadrilaterals and curvilinear interfaces.

4. Multiplier spaces for general quadrilaterals

In this section, we investigate the scalar case and remark that the extension to the vectorial case is straightforward. For the moment, we focus on one planar interface Γ, and ignore any potential necessity for modifications on $\partial\Gamma$. However, we allow that the interface grids $\mathcal{T}^{\mathrm{m}}$ and $\mathcal{T}^{\mathrm{s}}$ consist of general non-degenerate convex quadrilaterals or triangles. In case of parallelograms or triangles, the following considerations reduce to the already known standard case. The discrete Lagrange multiplier space M_h is simply defined as the span of all nodal basis functions μ_p^g, where p is a vertex of the slave side grid. As usual, each basis function μ_p^g is defined element-wise as

$$\mu_p^g = \sum_{T \in \mathcal{T}^p} \mu_p^T \tag{14}$$

with local supports $\mathcal{T}^p = \{T \in \mathcal{T}^{\mathrm{s}} : p \text{ is a vertex of } T\}$ for μ_p^g and T for μ_p^T. Here and in the sequel, we will abuse the notation and indicate by p either a global vertex of the triangulation or a local node number within an element T, depending on the context. Moreover, we will usually write μ_p instead of μ_p^T when there is no ambiguity involved. It is sufficient for the dual approach that the local multiplier functions μ_p satisfy a biorthogonality relation with the element basis functions ϕ_q^{s} of the trace space W_h^{s}, namely,

$$\int_T \mu_p \phi_q^{\mathrm{s}} \,\mathrm{d}T \;=\; \delta_{pq} \int_T \phi_q^{\mathrm{s}} \,\mathrm{d}T. \tag{15}$$

As usual, the integration of the left side of (15) is performed via a transformation to the reference element $\widehat{T}$. For a simplex T, the corresponding reference element $\widehat{T}$ is the triangle with vertices $(0,0)$, $(1,0)$, $(0,1)$, while for quadrilaterals, $\widehat{T}$ is set to be the unit square $(0,1)^2$. We remark that, within the considered setting, it is not sufficient to simply choose the Lagrange multiplier μ_p as $\widehat{\mu}_p \circ F_T^{-1}$ with $F_T : \widehat{T} \to T$ the element mapping and $\widehat{\mu}_p$ respecting a biorthogonality relation with the shape functions $\widehat{\phi}_q^{\mathrm{s}}$ on the reference element $\widehat{T}$. This is due to the fact that, for quadrilaterals, F_T is not necessarily an affine, i.e. $P1$-mapping, but an isoparametric $Q1$-mapping. This yields a surface element $\mathrm{d}T = |\det DF_T| \mathrm{d}\widehat{T}$ with a linear contribution $\det DF_T$. We note that the expression $\det DF_T$ abuses the notation since F_T maps from $\widehat{T} \subset \mathbb{R}^2$ to $\mathbb{R}^3$, and the Jacobian DF_T is not a square matrix. To be more specific, when F_T is written as $(u,v) \mapsto (x,y,z) = F_T(u,v)$, then we set $\det DF_T = \sqrt{EG - H^2}$ with $E = (\partial x/\partial u)^2 + (\partial y/\partial u)^2 + (\partial z/\partial u)^2$, $G = (\partial x/\partial v)^2 + (\partial y/\partial v)^2 + (\partial z/\partial v)^2$, $H = (\partial x/\partial u)(\partial x/\partial v) + (\partial y/\partial u)(\partial y/\partial v) + (\partial z/\partial u)(\partial z/\partial v)$. Transforming the required integral to the reference element, we obtain

$$\int_T \mu_p \phi_q^{\mathrm{s}} \,\mathrm{d}T \;=\; \int_{\widehat{T}} \widehat{\mu}_p \widehat{\phi}_q^{\mathrm{s}} |\det DF_T| \,\mathrm{d}\widehat{T}, \tag{16}$$

from which we obviously cannot expect that (15) is satisfied. In what follows, we will provide two alternative ways of defining M_h, both yielding (15). The first approach relies on the solution of local subproblems on each element, whereas the second one uses a special transformation to eliminate $|\det DF_T|$ from (16).

4.1. **Local subproblems.** We indicate by D_T and $M_T \in \mathbb{R}^{n_\mathrm{s}\times n_\mathrm{s}}$ the diagonal matrix and the element mass matrix, respectively, with entries given by

$$d_{pp} = \int_T \phi_p^\mathrm{s}\,\mathrm{d}T, \qquad m_{pq} = \int_T \phi_p^\mathrm{s}\phi_q^\mathrm{s}\,\mathrm{d}T.$$

With $A_T = D_T M_T^{-1}$, we define

$$\mu_p^T = \sum_q a_{pq}\phi_q^\mathrm{s}, \tag{17}$$

and obtain the biorthogonality (15) by

$$\int_T \mu_p\phi_q^\mathrm{s} = \sum_k a_{pk}m_{kq} = (A_T M_T)_{pq} = d_{pq} = \delta_{pq}\int_T \phi_q^\mathrm{s}\,\mathrm{d}T.$$

Above and in the sequel, we always assume that the summation index runs from 1 to n_s, the number of element vertices, unless another index set is given. We continue by showing that the global space M_h constructed in this way contains the constant functions. Then, by using the L^2-stability of the mortar-projection, it can be easily shown that M_h satisfies an approximation property.

Lemma 1. *Let M_h be constructed from* (14) *and* (17). *Then $\mathbb{P}_0 \subset M_h$.*

Proof. Denoting by $\mathcal{V}^\mathrm{s}$ the set of vertices of $\mathcal{T}^\mathrm{s}$, and by $\mathbf{1} \in \mathbb{R}^{n_\mathrm{s}}$ the vector of unity, we observe that

$$\sum_{p\in\mathcal{V}^\mathrm{s}} \mu_p^g|_T = \sum_p \mu_p = \sum_{p,q} a_{pq}\phi_q^\mathrm{s} = \sum_q (A_T^\mathrm{T}\mathbf{1})_q\phi_q^\mathrm{s} = \sum_q (M_T^{-1}D_T\mathbf{1})_q\phi_q^\mathrm{s}. \tag{18}$$

A simple calculation reveals that $M_T^{-1}D_T\mathbf{1} = \mathbf{1}$, namely for $b = M_T^{-1}D_T\mathbf{1} - \mathbf{1}$, we have that

$$(M_T b)_p = (D_T\mathbf{1} - M_T\mathbf{1})_p = \int_T \phi_p^\mathrm{s}\,\mathrm{d}T - \int_T \phi_p^\mathrm{s}\sum_q \phi_q^\mathrm{s}\,\mathrm{d}T = 0,$$

thus, $M_T b = 0$ yielding $b = 0$. From (18), we get that

$$\sum_{p\in\mathcal{V}^\mathrm{s}} \mu_p^g|_T = \sum_q \mathbf{1}_q\phi_q^\mathrm{s} = \sum_q \phi_q^\mathrm{s} = 1,$$

which concludes the proof. □

We note that the entries of the global coupling matrix M can be easily assembled by the local contributions of $(M_\mathrm{sm})_{pq} = \int_{T^\mathrm{sm}} \phi_p^\mathrm{s}\phi_q^\mathrm{m}\,\mathrm{d}T^\mathrm{sm}$, where T^sm denotes the intersection of a slave and a master element. Formally, this gives

$$M = \sum_{T^\mathrm{sm}=T^\mathrm{s}\cap T^\mathrm{m}} R_{T^\mathrm{s}} D_{T^\mathrm{s}} M_{T^\mathrm{s}}^{-1} M_\mathrm{sm} R_{T^\mathrm{m}}^\mathrm{T},$$

where R_{T^k} denotes the matrix which maps the local node numbers of the element T^k to the global ones with respect to $\mathcal{T}^k$, $k = \mathrm{m}, \mathrm{s}$.

4.2. **Special transformation.** In the previous subsection, a local mass matrix has to be inverted on each element for the construction of the dual Lagrange multipliers. Here, we introduce an alternative procedure for deriving them. They are given in terms of a special transformation from the reference element, namely, by

$$\mu_p^T = \frac{w_p}{|\det DF_T|}\widehat{\mu}_p \circ F_T^{-1}, \tag{19}$$

with a weighting factor $w_p = (\int_T \phi_p^\mathrm{s}\,\mathrm{d}T)/(\int_{\widehat{T}} \widehat{\phi}_p^\mathrm{s}\,\mathrm{d}\widehat{T})$. In case of a planar interface, the factors $w_p/|\det DF_T|$ are equal to 1, and the approach reduces to the original one. As before, the construction almost immediately implies (15) by observing that

$$\int_T \mu_p\phi_q^\mathrm{s}\,\mathrm{d}T = w_p\int_{\widehat{T}} \widehat{\mu}_p\widehat{\phi}_q^\mathrm{s}\,\mathrm{d}\widehat{T} = \delta_{pq}\int_T \phi_p^\mathrm{s}\,\mathrm{d}T.$$

Again, we verify the approximation property of M_h by showing that it contains the constants.

Lemma 2. *Let M_h be constructed from* (14) *and* (19). *Then $\mathbb{P}_0 \subset M_h$.*

Proof. We take $\mu = \sum_{p\in\mathcal{V}^{\mathrm{s}}} \mu_p^g|_T = \sum_p \mu_p$. We first consider the fact that

$$\mu = 1 \Leftrightarrow \widehat{\mu} = 1 \text{ with } \widehat{\mu} = \mu \circ F_T = \sum_p \frac{w_p}{|\det DF_T|}\widehat{\mu}_p.$$

Moreover, it holds that both $|\det DF_T|\widehat{\mu}$ and $|\det DF_T|$ are $Q1$-functions. We can verify the assertion by showing that $|\det DF_T|\widehat{\mu} = |\det DF_T|$, which is in this case equivalent to the requirement that

$$I = \int_{\widehat{T}} (|\det DF_T|\widehat{\mu} - |\det DF_T|)\widehat{\phi}_q^{\mathrm{s}}\,\mathrm{d}\widehat{T} = 0, \quad q = 1, \ldots, n_{\mathrm{s}}.$$

Using the biorthogonality on $\widehat{T}$ and the definition of the weights w_p, we obtain

$$\begin{aligned} I &= \int_{\widehat{T}} \sum_p w_p\widehat{\mu}_p\widehat{\phi}_q^{\mathrm{s}}\,\mathrm{d}\widehat{T} - \int_{\widehat{T}} \widehat{\phi}_q^{\mathrm{s}}|\det DF_T|\,\mathrm{d}\widehat{T} \\ &= \int_{\widehat{T}} \left(\frac{\int_T \phi_q^{\mathrm{s}}\,\mathrm{d}T}{\int_{\widehat{T}} \widehat{\phi}_q^{\mathrm{s}}\,\mathrm{d}\widehat{T}}\right) \widehat{\phi}_q^{\mathrm{s}}\,\mathrm{d}\widehat{T} - \int_T \phi_q^{\mathrm{s}}\,\mathrm{d}T = 0, \end{aligned}$$

which concludes the proof. □

We remark that the implementation of the coupling matrix M does not require the inverse of a local mass matrix. It can be carried out by transferring μ_p and ϕ_q^{m} onto the reference element, i.e.,

$$\int_{T^{\mathrm{sm}}} \mu_p\phi_q^{\mathrm{m}}\,\mathrm{d}T^{\mathrm{sm}} = w_p \int_{\widehat{T}^{\mathrm{sm}}} \widehat{\mu}_p(\phi_q^{\mathrm{m}} \circ F_T)\,\mathrm{d}\widehat{T}^{\mathrm{sm}}$$

4.3. **Numerical results.** The theoretical results of Subsections 4.1 and 4.2 yield optimal a priori estimates for the error in the broken H^1-norm. Here, we are interested in the quantitative numbers. In addition to the two approaches considered above, we employ two other methods for comparison: one using standard basis functions $\mu_p = \phi_p^{\mathrm{s}}$ not satisfying (15), and a "naive" one, where μ_p is chosen as $\widehat{\mu}_p \circ F_T^{-1}$ for the coupling with the master side, but it is set to be $(|T|/|\det DF_T|)\widehat{\mu}_p \circ F_T^{-1}$ for the coupling with the slave side. We note that the latter approach satisfies (15), and coincides with the original dual method for simplices and parallelepipeds. The choice is motivated by the fact that nothing has to be modified for the coupling on the master side, and only a minimal modification is necessary for the coupling on the slave side. However, despite its similarity with (19), constants are not preserved due to the choice of $|T|$ as weights. Therefore, the approximation property is lost, and optimal convergence cannot be guaranteed anymore.

We consider a simple test example with two cubes Ω^{m} and Ω^{s} of length and width 1 and height 0.2, sharing as interface the unit square of edge length 1 at $z = 0$. We solve (6) with right hand side f derived from the exact solution $u(x, y, z) = yz\mathrm{e}^{-x^2}$. On the planes $z = \pm 0.2$, Dirichlet boundary data is considered, while on the remaining part of the boundary, we employ Neumann data. The Lagrange multiplier space M_h is associated with the grid on the lower cube. For the surface meshes $\mathcal{T}^{\mathrm{s}}$ on the slave side, we compare three different sequences as in [1]: square, asymptotically parallelogram, and trapezoidal, see Figure 1. For the first two sequences, the initial triangulation is indicated by thick lines, and the subsequent grids are simply obtained by uniform refinements. For the trapezoidal grids, the same initial triangulation as for the asymptotically parallelogram grid is used, but instead of employing a standard uniform refinement procedure, the surface is partitioned into congruent trapezoids at each step , all similar to the trapezoid with vertices $(0, 0)$, $(0.5, 0)$, $(0.5, 0.2)$, and $(0, 0.8)$. The thin lines in the pictures of Figure 1 indicate the slave side grids after two refinements. On the master side, the meshes $\mathcal{T}^{\mathrm{m}}$ consist of squares twice the size of the elements on the slave side.

In Figure 2, the error decays measured in the H^1-norm are plotted for different grid sequences and different Lagrange multipliers. In particular, we compare three approaches: the naive dual one

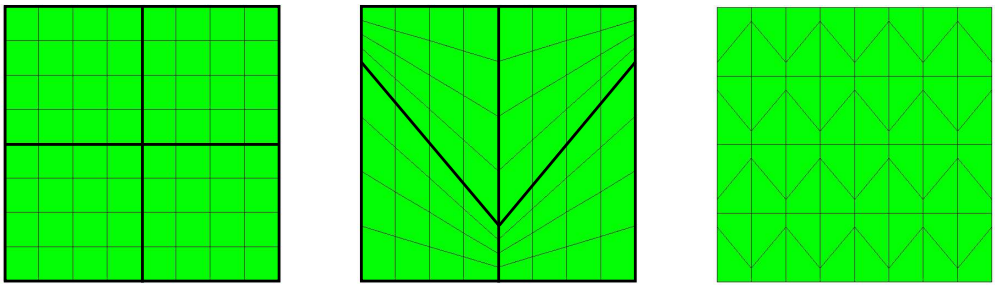

FIGURE 1. Surface grids $\mathcal{T}^{\mathrm{s}}$: square (left), asymptotically parallelogram (middle), trapezoidal (right).

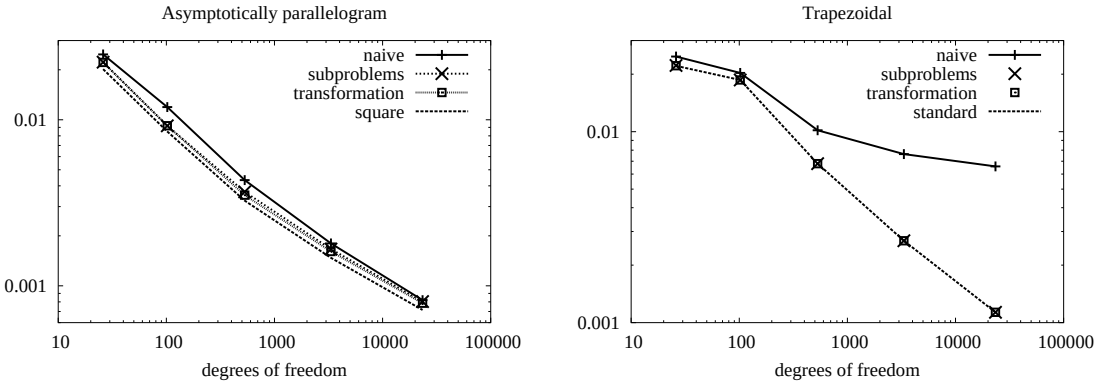

FIGURE 2. Error decays, measured in the H^1-norm: asymptotically parallelogram (left) and trapezoidal (right).

and the ones introduced in Sections 4.1 and 4.2. For the asymptotically parallelogram grid sequence illustrated in the left picture, we choose the results from the uniform square grids as reference. All approaches give qualitatively the same and quantitatively almost the same results. This observation changes drastically when employing the sequence of trapezoidal grids, as illustrated in the right picture. The naive approach fails completely, the error remains almost static after a few refinement steps. The other two methods behave as predicted by the theory. Moreover, the errors visually coincide with the approach using standard basis function which is taken as a reference here.

5. Modifications for curved interfaces

Our numerical results above illustrate how sensitive the quality of the mortar approximation depends on the choice of the Lagrange multiplier space. In this section, we consider variational crimes resulting from curvilinear interfaces. We extend our results of the 2D scalar, [7], and vectorial case, [8], to dimension $d \in \{2, 3\}$. We focus on the case of vector fields. In general, the surface grids $\mathcal{T}^{\mathrm{m}}$ and $\mathcal{T}^{\mathrm{s}}$ cannot resolve a curvilinear interface Γ. Geometrically, they form piecewise $P1$ or $Q1$ interpolations Γ_h^{m} and Γ_h^{s} of the exact interface Γ. The meshes from both sides can partially overlap or even exhibit gaps. Therefore, in order to pose a discrete problem formulation, the coupling bilinear form $b(\cdot,\cdot)$ given by (2) has to be suitably approximated by a form $b_h(\cdot,\cdot) : X_h \times M_h \to \mathbb{R}$. For the coupling of the Lagrange multipliers with the slave side, no modifications are necessary, since the corresponding functions are all associated with the same triangulation $\mathcal{T}^{\mathrm{s}}$. However, the coupling with the master side is much more involved. As in [8], we define a suitable linear and stable projection operator P_{s} onto the slave side,

$$P_{\mathrm{s}} : (L^2(\Gamma_h^{\mathrm{m}}))^d \to (L^2(\Gamma_h^{\mathrm{s}}))^d, \quad \boldsymbol{v}_{\mathrm{m}} \mapsto P_{\mathrm{s}}\boldsymbol{v}_{\mathrm{m}}, \tag{20}$$

a mesh dependent jump $[\cdot]_h$ by

$$[\boldsymbol{v}]_h = \boldsymbol{v}_{\mathrm{s}} - P_{\mathrm{s}}\boldsymbol{v}_{\mathrm{m}},$$

and the approximate coupling bilinear form $b_h(\cdot,\cdot)$ as

$$b_h(\boldsymbol{v},\boldsymbol{\mu}) = (\,[\boldsymbol{v}]_h,\,\boldsymbol{\mu}\,)_{L^2(\Gamma_h^{\mathrm{s}})}, \quad (\boldsymbol{v},\boldsymbol{\mu}) \in X_h \times M_h. \tag{21}$$

In [7], we show that the analogous approach for the scalar case yields optimal a priori estimates. These estimates can be transfered to the vectorial case by standard arguments. However, for the vectorial case, if dual Lagrange multipliers are chosen with respect to the coarse grid, one can observe a preasymptotic misbehavior in form of unwanted oscillations, even for a very simple linear elasticity model problem, see [8]. There, we present a remedy for the two-dimensional case which preserves the advantages of the dual approach. In the following, we present two alternatives for dimension $d \in \{2,3\}$. Both have in common that only the coupling of the Lagrange multipliers to the master side is changed, namely, $(P_{\mathrm{s}}\boldsymbol{v}_{\mathrm{m}},\,\boldsymbol{\mu})_{L^2(\Gamma_h^{\mathrm{s}})}$. To this end, the coupling bilinear form $b_h(\cdot,\cdot)$ is replaced by a modification $b_h^{\mathrm{mod}}(\cdot,\cdot)$. In the first alternative to be given, we replace the L^2-scalar product $(\cdot,\cdot)_{L^2(\Gamma_h^{\mathrm{s}})}$ by a discrete one, whereas in the second alternative the Lagrange multiplier $\boldsymbol{\mu} \in M_h$ as seen by the master side is replaced by $\boldsymbol{\mu} + \Delta\boldsymbol{\mu}$. Both approaches reduce to the original one in the case of a planar interface.

Before we introduce the two modifications, we address some common issues which are needed for deriving them. With each node p on the smooth interface Γ, an orthonormal basis $B_p \in \mathbb{R}^{d\times d}$ is associated, given by

$$B_p = (\boldsymbol{b}_p^{(1)}, \ldots, \boldsymbol{b}_p^{(d)}) \tag{22}$$

with $\boldsymbol{b}_p^{(1)} = \boldsymbol{n}_p$ being the unit normal vector on Γ in p, and the remaining columns being corresponding unit tangent vectors. In the following $\boldsymbol{n}_p$ can be the exact normal on Γ or a weighted sum of the face normals sharing the node p. In the case that Γ is piecewise smooth, we have to decompose Γ into smooth non-overlapping subsets, the boundaries of which have to be regarded as wire-basket edges.

Our modifications will be given in terms of the difference of two bases B_p, B_q, where p refers to a slave node, and, in Section 5.1, B_q is associated with a master node such that the supports of the corresponding basis functions intersect, whereas in Section 5.2, the nodes p and q are both vertices of one slave side element. For the upcoming analysis in both cases, we assume that

$$\|B_p - B_q\|_\infty = O(h), \tag{23}$$

provided that $\|\boldsymbol{p} - \boldsymbol{q}\|_\infty = O(h)$ where $\boldsymbol{p}$ and $\boldsymbol{q}$ are the coordinate vectors of the nodes p and q, respectively. For the first column of B_p and B_q, namely, the difference of the normal vectors $\boldsymbol{n}_p$ and $\boldsymbol{n}_q$, this is an obvious fact. Whereas in two dimensions, the choice of the tangent vector is unique up to the sign (and fixing this choice yields the required property), the construction of two vectors spanning the tangent plane in three dimensions is by no means unique. However, if Γ is not a closed surface, it is easily possible to define the tangent vectors in an unambiguous and continuous way. To this end, we fix one orthonormal system B_* and require that the difference of the first column $\boldsymbol{b}_*^{(1)}$ and any normal vector $\boldsymbol{n}_p$ on Γ is bounded from below by a constant. Then, for each vertex p, the basis B_p can be defined in terms of the unique Householder reflection $H_p \in \mathbb{R}^{d\times d}$ mapping $\boldsymbol{b}_*^{(1)}$ onto $\boldsymbol{n}_p$, namely, $B_p = H_p B_*$. We remark that the choice of $\boldsymbol{b}_*^{(1)}$ avoids any errors due to cancellation. For the sake of clarity, we will indicate by $B_{p,\mathrm{s}}$ or $B_{p,\mathrm{m}}$ whether the node p is associated with the slave or the master side, respectively.

5.1. **Point-wise algebraic modification.** In order to motivate our choice for the point-wise modification, we note that the discrete system (4) is for $\lambda_{\mathrm{s}} = \lambda_h$ and $D_{\mathrm{s}} = D$ equivalent to

$$\begin{pmatrix} A_{\mathrm{ii}} & A_{\mathrm{im}} & A_{\mathrm{is}} & 0 & 0 \\ A_{\mathrm{mi}} & A_{\mathrm{mm}} & 0 & 0 & D_{\mathrm{m}}^{\mathrm{T}} \\ A_{\mathrm{si}} & 0 & A_{\mathrm{ss}} & D_{\mathrm{s}}^{\mathrm{T}} & 0 \\ 0 & -M & D_{\mathrm{s}} & 0 & 0 \\ 0 & 0 & 0 & M^{\mathrm{T}} & D_{\mathrm{m}} \end{pmatrix} \begin{pmatrix} u_h^{\mathrm{i}} \\ u_h^{\mathrm{m}} \\ u_h^{\mathrm{s}} \\ \lambda_{\mathrm{s}} \\ \lambda_{\mathrm{m}} \end{pmatrix} = \begin{pmatrix} f^{\mathrm{i}} \\ f^{\mathrm{m}} \\ f^{\mathrm{s}} \\ 0 \\ 0 \end{pmatrix}. \tag{24}$$

The system above admits the definition of a discrete dual Lagrange multiplier on the master side by

$$\lambda_{\mathrm{m}} = -D_{\mathrm{m}}^{-1} M^{\mathrm{T}} \lambda_{\mathrm{s}}, \tag{25}$$

where the entries of the diagonal matrix D_{m} are given by $\int_{\Gamma_h^{\mathrm{m}}} \phi_q^{\mathrm{m}} \, \mathrm{d}\Gamma_h^{\mathrm{m}}$. Formally, (24) corresponds to a three field approach. The fluxes λ_{m} and λ_{s} satisfy a weak continuity condition. We refer to [5] for more details. From (25), it can be seen that a Lagrange multiplier λ_{s} on the slave side which is constant in normal direction, yields a multiplier λ_{m} on the master side which does not necessarily possess this property. For the 2D case, this lack of preservation is identified as the reason for the misbehavior of the dual Lagrange multipliers, see [8]. Our first modification will replace M in (25) by a matrix M^{mod}, such that quantities constant in normal direction are preserved.

5.1.1. *Formulation.* In the case of curvilinear interfaces, we cannot preserve quantities being constant in normal direction and at the same time quantities being constant with respect to a fixed coordinate system. This observation motivates our choice that we work with a non-symmetric Petrov–Galerkin scheme, where we replace M in the last line of (24) by the modified matrix

$$M^{\mathrm{mod}} = B_{\mathrm{s}} M B_{\mathrm{m}}^{\mathrm{T}}, \tag{26}$$

where $B_{\mathrm{s}} \in \mathbb{R}^{N_{\mathrm{s}} d \times N_{\mathrm{s}} d}$ and $B_{\mathrm{m}} \in \mathbb{R}^{N_{\mathrm{m}} d \times N_{\mathrm{m}} d}$ are the block diagonal matrices with entries $B_{p,\mathrm{s}}$ and $B_{q,\mathrm{m}}$, respectively, i.e., each block consists of an orthonormal basis with one basis vector being the unit normal vector associated with the corresponding node. By N_k, we indicate the total number of finite element nodes on $\mathcal{T}^k$, $k = \mathrm{m}, \mathrm{s}$. We note that D_{m} has the same block structure as B_{m} with $(d \times d)$-blocks of the form $s\mathrm{Id}$, $s \in \mathbb{R}$. Therefore, we have that $D_{\mathrm{m}}^{-1} B_{\mathrm{m}} = B_{\mathrm{m}} D_{\mathrm{m}}^{-1}$, yielding

$$\lambda_{\mathrm{m}} = -D_{\mathrm{m}}^{-1} (B_{\mathrm{s}} M B_{\mathrm{m}}^{\mathrm{T}})^{\mathrm{T}} \lambda_{\mathrm{s}} = -B_{\mathrm{m}} D_{\mathrm{m}}^{-1} M^{\mathrm{T}} B_{\mathrm{s}}^{\mathrm{T}} \lambda_{\mathrm{s}},$$

which gives

$$B_{\mathrm{m}}^{\mathrm{T}} \lambda_{\mathrm{m}} = -D_{\mathrm{m}}^{-1} M^{\mathrm{T}} B_{\mathrm{s}}^{\mathrm{T}} \lambda_{\mathrm{s}}.$$

We note that the application of the rotation $B_{\mathrm{s}}^{\mathrm{T}}$ to the coefficient vector λ_{s} yields the components in normal direction and with respect to the tangent plane in each node. Thus, if λ_{s} is constant in a discrete way in normal direction and with respect to the tangent planes, we have that $B_{\mathrm{s}}^{\mathrm{T}} \lambda_{\mathrm{s}} \in \mathbb{R}^{N_{\mathrm{s}} d}$ can be written as $c_{\mathrm{s}} = (\boldsymbol{a}^{\mathrm{T}}, \dots, \boldsymbol{a}^{\mathrm{T}})^{\mathrm{T}}$ with $\boldsymbol{a} \in \mathbb{R}^d$. Additionally observing that $D_{\mathrm{m}} c_{\mathrm{m}} = M^{\mathrm{T}} c_{\mathrm{s}} \in \mathbb{R}^{N_{\mathrm{m}} d}$ with $c_{\mathrm{m}} = (\boldsymbol{a}^{\mathrm{T}}, \dots, \boldsymbol{a}^{\mathrm{T}})^{\mathrm{T}}$, we conclude with

$$B_{\mathrm{s}}^{\mathrm{T}} \lambda_{\mathrm{s}} = c_{\mathrm{s}} \quad \Leftrightarrow \quad B_{\mathrm{m}}^{\mathrm{T}} \lambda_{\mathrm{m}} = c_{\mathrm{m}} \tag{27}$$

Thus, the modification (26) guarantees that the normal and tangential components of a vector field are transfered correctly between the master and the slave side in the sense of (27).

5.1.2. *Analysis.* We note that the mass matrix M in the fourth line of (24) is kept. Thus for the primal variable, we preserve constants with respect to a fixed coordinate system whereas for the dual variable constants with respect to the normal direction are preserved across the interface. The key for the analysis of the resulting modified discrete problem formulation is to suitably relate the two constrained spaces

$$\begin{aligned} V_h &= \{\boldsymbol{v} \in X_h : b_h(\boldsymbol{v}, \boldsymbol{\mu}) = 0, \ \boldsymbol{\mu} \in M_h\}, \\ V_h^{\mathrm{mod}} &= \{\boldsymbol{v} \in X_h : b_h^{\mathrm{mod}}(\boldsymbol{v}, \boldsymbol{\mu}) = 0, \ \boldsymbol{\mu} \in M_h\}. \end{aligned}$$

Lemma 3. *Let the modification be given by* (26)*. Then, for an arbitrary $\boldsymbol{v} = (\boldsymbol{v}_m, \boldsymbol{v}_s) \in V_h$, there exists $\Delta \boldsymbol{v} \in X_h$ such that*

$$\boldsymbol{v}^{\mathrm{mod}} = \boldsymbol{v} + \Delta \boldsymbol{v} \in V_h^{\mathrm{mod}}, \tag{28a}$$

$$\|\Delta \boldsymbol{v}\|_{X_h} \leq C h^{1/2} \|\boldsymbol{v}_m\|_{X_h}, \tag{28b}$$

$$\|\Delta \boldsymbol{v}\|_{0,\Gamma_h^s} \leq C h |\boldsymbol{v}_m|_{0,\Gamma_h^m}, \tag{28c}$$

$$\|\boldsymbol{v}\|_{X_h} \sim \|\boldsymbol{v}^{\mathrm{mod}}\|_{X_h}, \qquad h \text{ small enough.} \tag{28d}$$

The analogous statement holds for arbitrary $\boldsymbol{v}^{\mathrm{mod}} \in V_h^{\mathrm{mod}}$.

Proof. In terms of the scalar basis functions μ_p, the space V_h can be written as

$$V_h \;=\; \{\boldsymbol{v} \in X_h : (\mu_p, [\boldsymbol{v}]_h)_{L^2(\Gamma_h^{\mathrm{s}})} = \boldsymbol{0},\; p \in \mathcal{V}^{\mathrm{s}}\}$$

For $\boldsymbol{v} = (\boldsymbol{v}_{\mathrm{m}}, \boldsymbol{v}_{\mathrm{s}}) \in X_h$ with $\boldsymbol{v}_{\mathrm{m}} = \sum_{q\in\mathcal{V}^{\mathrm{m}}} \boldsymbol{\alpha}_q^{\mathrm{m}} \phi_q^{\mathrm{m}}$, $\boldsymbol{v}_{\mathrm{s}} = \sum_{q\in\mathcal{V}^{\mathrm{s}}} \boldsymbol{\beta}_q^{\mathrm{s}} \phi_q^{\mathrm{s}}$, we deduce from (26) that

$$V_h^{\mathrm{mod}} \;=\; \left\{ \boldsymbol{v} \in X_h : \left(\mu_p, \boldsymbol{v}_{\mathrm{s}} - \sum_{q\in\mathcal{V}^{\mathrm{m}}} Q_{pq} \boldsymbol{\alpha}_q^{\mathrm{m}} P_{\mathrm{s}} \phi_q^{\mathrm{m}} \right)_{L^2(\Gamma_h^{\mathrm{s}})} = \boldsymbol{0},\; p \in \mathcal{V}^{\mathrm{s}} \right\}$$

with $Q_{pq} = B_{p,\mathrm{s}} B_{q,\mathrm{m}}^{\mathrm{T}}$. We note that, in terms of the reference orthonormal basis B_* and the Householder reflections H_p and H_q introduced above, we have that

$$Q_{pq} = B_{p,\mathrm{s}} B_{q,\mathrm{m}}^{\mathrm{T}} = H_p B_* B_*^{\mathrm{T}} H_q^{\mathrm{T}} = H_p H_q, \tag{29}$$

thus, Q_{pq} is the rotation matrix which maps the orthonormal system $B_{q,\mathrm{m}}$ to the system $B_{p,\mathrm{s}}$. In the special case of a planar interface, Q_{pq} is the identity for all nodes and thus $V_h = V_h^{\mathrm{mod}}$. For $\boldsymbol{v} \in V_h$, we define $\Delta\boldsymbol{v} \in X_h$ by

$$\Delta\boldsymbol{v} \;=\; \left(0\,,\; \sum_{p\in\mathcal{V}^{\mathrm{s}}} \boldsymbol{\gamma}_p \phi_p^{\mathrm{s}} \right), \quad \boldsymbol{\gamma}_p = \frac{\left(\mu_p,\; P_{\mathrm{s}} \left(\sum_{q\in\mathcal{V}^{\mathrm{m}}} (Q_{pq} - \mathrm{Id}) \boldsymbol{\alpha}_q^{\mathrm{m}} \phi_q^{\mathrm{m}} \right) \right)_{L^2(\Gamma_h^{\mathrm{s}})}}{(\phi_p^{\mathrm{s}},\; \mu_p)_{L^2(\Gamma_h^{\mathrm{s}})}}. \tag{30}$$

Using the duality (5), it is easy to see that $\boldsymbol{v}^{\mathrm{mod}} = \boldsymbol{v} + \Delta\boldsymbol{v} \in V_h^{\mathrm{mod}}$. In particular,

$$\begin{aligned}
&\left(\mu_p, \sum_{q\in\mathcal{V}^{\mathrm{s}}} (\boldsymbol{\beta}_q^{\mathrm{s}} + \boldsymbol{\gamma}_q^{\mathrm{s}}) \phi_q^{\mathrm{s}} - P_{\mathrm{s}} \left(\sum_{q\in\mathcal{V}^{\mathrm{m}}} Q_{pq} \boldsymbol{\alpha}_q^{\mathrm{m}} \phi_q^{\mathrm{m}} \right) \right)_{L^2(\Gamma_h^{\mathrm{s}})} \\
&\;=\; \boldsymbol{\gamma}_p (\phi_p^{\mathrm{s}},\, 1)_{L^2(\Gamma_h^{\mathrm{s}})} \;+\; \left(\mu_p, \boldsymbol{v}_{\mathrm{s}} - P_{\mathrm{s}} \left(\sum_{q\in\mathcal{V}^{\mathrm{m}}} Q_{pq} \boldsymbol{\alpha}_q^{\mathrm{m}} \phi_q^{\mathrm{m}} \right) \right)_{L^2(\Gamma_h^{\mathrm{s}})} \\
&\;=\; (\mu_p, \boldsymbol{v}_{\mathrm{s}} - P_{\mathrm{s}} \boldsymbol{v}_{\mathrm{m}})_{L^2(\Gamma_h^{\mathrm{s}})} \;=\; 0.
\end{aligned}$$

Using the equivalence of discrete norms and scaling arguments, (30) implies that

$$\|\Delta\boldsymbol{v}\|_{X_h}^2 \le C h^{d-2} \sum_{p\in\mathcal{V}^{\mathrm{s}}} |\boldsymbol{\gamma}_p|^2, \tag{31a}$$

$$\|\Delta\boldsymbol{v}\|_{0,\Gamma_h^{\mathrm{s}}}^2 \le C h^{d-1} \sum_{p\in\mathcal{V}^{\mathrm{s}}} |\boldsymbol{\gamma}_p|^2. \tag{31b}$$

An estimation of the coefficients $\boldsymbol{\gamma}_p$ gives

$$|\boldsymbol{\gamma}_p|^2 \;\le\; C \sum_{q\in\mathcal{V}^{p,\mathrm{m}}} |\boldsymbol{\alpha}_q^{\mathrm{m}}|^2 \|Q_{pq} - \mathrm{Id}\|_\infty^2,$$

where $\mathcal{V}^{p,\mathrm{m}}$ denotes the set of all master nodes q such that $\operatorname{supp}\mu_p \cap \operatorname{supp}\phi_q^{\mathrm{m}}$ has positive $(d-1)$-dimensional measure. Considering (29) and the fact that $B_{p,\mathrm{s}} = O(1)$, together with applying assumption (23), yields

$$\|Q_{pq} - \mathrm{Id}\|_\infty^2 = \|B_{p,\mathrm{s}} B_{q,\mathrm{m}}^{\mathrm{T}} - \mathrm{Id}\|_\infty^2 = \|B_{p,\mathrm{s}} (B_{q,\mathrm{m}}^{\mathrm{T}} - B_{p,\mathrm{s}}^{\mathrm{T}})\|_\infty^2 = O(h^2).$$

Summing up, we obtain

$$\sum_{p\in\mathcal{V}^{\mathrm{s}}} |\boldsymbol{\gamma}_p|^2 \;\le\; C h^2 \sum_{q\in\mathcal{V}^{\mathrm{m}}} |\boldsymbol{\alpha}_q^m|^2$$

By the same considerations as above, we have

$$\sum_{q\in\mathcal{V}^{\mathrm{m}}} |\boldsymbol{\alpha}_q^m|^2 \;\le\; C h^{1-d} \|\boldsymbol{v}_{\mathrm{m}}\|_{0,\Gamma_h^{\mathrm{m}}}^2,$$

and, therefore, taking into account (31),

$$\|\Delta\boldsymbol{v}\|_{X_h}^2 \le C h \|\boldsymbol{v}_{\mathrm{m}}\|_{X_h}^2, \quad \text{and} \quad \|\Delta\boldsymbol{v}\|_{0,\Gamma_h^{\mathrm{s}}}^2 \le C h^2 \|\boldsymbol{v}_{\mathrm{m}}\|_{0,\Gamma_h^{\mathrm{m}}}^2,$$

yielding (28b) and (28c). The norm equivalence (28d) follows from (28b) by observing that

$$\|\boldsymbol{v}\|_{X_h} \begin{cases} \geq \|\boldsymbol{v}^{\mathrm{mod}}\|_{X_h} - \|\Delta\boldsymbol{v}\|_{X_h} \geq (1 - Ch^{1/2})\|\boldsymbol{v}^{\mathrm{mod}}\|_{X_h}, \\ \leq \|\boldsymbol{v}^{\mathrm{mod}}\|_{X_h} + \|\Delta\boldsymbol{v}\|_{X_h} \leq (1 + Ch^{1/2})\|\boldsymbol{v}^{\mathrm{mod}}\|_{X_h}, \end{cases}$$

provided that h is small enough. According to (30), we observe that $\Delta\boldsymbol{v}$ only depends on $\boldsymbol{v}_{\mathrm{m}} = \boldsymbol{v}_{\mathrm{m}}^{\mathrm{mod}}$. Therefore, it is obvious that the analogous statement of the Lemma has to hold for an arbitrary $\boldsymbol{v}^{\mathrm{mod}} \in V_h^{\mathrm{mod}}$. □

Unfortunately, Lemma 3 only admits a suboptimal approximation property for the constrained space V_h^{mod}. We recall that a translation which is a rigid body motion in linear elasticity is not in V_h^{mod}. However, it is possible to derive optimal a priori estimates by considering the non-symmetric Petrov–Galerkin approach, namely, to find $\boldsymbol{u}_h \in V_h$ such that

$$a_h(\boldsymbol{u}_h, \boldsymbol{v}) = f_h(\boldsymbol{v}), \qquad \boldsymbol{v} \in V_h^{\mathrm{mod}}.$$

For the above formulation, the approximation property is a standard result. It remains to prove the wellposedness and to estimate the consistency error. We remark that Lemma 3 implies that $\dim V_h^{\mathrm{mod}} = \dim V_h$, and, therefore, it is sufficient to prove the following lemma for showing wellposedness, [6].

Lemma 4. *Provided that h is small enough, there exists α such that*

$$\inf_{\boldsymbol{w}\in V_h} \sup_{\boldsymbol{v}\in V_h^{mod}} \frac{a_h(\boldsymbol{w}, \boldsymbol{v})}{\|\boldsymbol{w}\|_{X_h}\|\boldsymbol{v}\|_{X_h}} \;\geq\; \alpha.$$

Proof. For $\boldsymbol{w} \in V_h$, set $\boldsymbol{v} = \boldsymbol{w} + \Delta\boldsymbol{w} \in V_h^{\mathrm{mod}}$ with $\Delta\boldsymbol{w}$ given by Lemma 3. This yields

$$\begin{aligned} a_h(\boldsymbol{w}, \boldsymbol{v}) \;&=\; a_h(\boldsymbol{w}, \boldsymbol{w}) + a_h(\boldsymbol{w}, \Delta\boldsymbol{w}) \\ &\geq\; \alpha\|\boldsymbol{w}\|_{X_h}^2 - C\|\boldsymbol{w}\|_{X_h}\|\Delta\boldsymbol{w}\|_{X_h} \\ &\geq\; (\alpha - Ch^{1/2})\|\boldsymbol{w}\|_{X_h}^2, \end{aligned}$$

which gives the desired condition provided that h is small enough. □

For the estimation of the consistency error, we restrict ourselves to give the main arguments involving the modification. In particular, we ignore for the moment that an arbitrary function $\boldsymbol{v} \in X_h$ may not be properly defined on the curved interface Γ. We refer to [7] for a mathematically rigorous analysis.

Lemma 5. *For h small enough, it holds that*

$$\sup_{\boldsymbol{v}^{\mathrm{mod}}\in V_h^{\mathrm{mod}}} \frac{b(\boldsymbol{v}^{\mathrm{mod}}, \boldsymbol{\lambda})}{\|\boldsymbol{v}^{\mathrm{mod}}\|_{X_h}} \;\leq\; Ch\|\boldsymbol{u}\|_{2,\Omega}. \tag{32}$$

Proof. Using the bound for the consistency error for V_h and applying Lemma 3 yield for $\boldsymbol{v}^{\mathrm{mod}} \in V_h^{\mathrm{mod}}$

$$\begin{aligned} b(\boldsymbol{v}^{\mathrm{mod}}, \boldsymbol{\lambda}) \;&=\; (\boldsymbol{\lambda}, [\boldsymbol{v}^{\mathrm{mod}}])_{L^2(\Gamma)} \;=\; (\boldsymbol{\lambda}, [\boldsymbol{v}])_{L^2(\Gamma)} + (\boldsymbol{\lambda}, [\Delta\boldsymbol{v}])_{L^2(\Gamma)} \\ &\leq\; Ch\|\boldsymbol{v}\|_{X_h}|\boldsymbol{\lambda}|_{1/2,\Gamma} \;+\; \|\boldsymbol{\lambda}\|_{0,\Gamma}\|[\Delta\boldsymbol{v}]\|_{0,\Gamma}. \end{aligned}$$

Using (31b) and (28b), we obtain that

$$\|[\Delta\boldsymbol{v}]\|_{0,\Gamma} \leq Ch\|\boldsymbol{v}\|_{X_h},$$

yielding

$$b(\boldsymbol{v}^{\mathrm{mod}}, \boldsymbol{\lambda}) \;\leq\; Ch\left(|\boldsymbol{\lambda}|_{1/2,\Gamma} + \|\boldsymbol{\lambda}\|_{0,\Gamma}\right)\|\boldsymbol{v}\|_{X_h}$$

Together with the norm equivalence (28d), we get the desired result. □

We note that the implementation of this modification can be easily carried out. In addition to M, we only have to compute for each node q on the slave and on the master side the local matrices B_q.

5.2. **Momentum preserving modification.** Working with a symmetric formulation in the previous section, we cannot preserve translations. Moreover for the symmetric approach only sub-optimal a priori estimates can be shown. This results from the fact that we use a point-wise modification which does not show L^2-stability. The modification $b_h^{\mathrm{mod}}(\cdot,\cdot)$ can be also interpreted by replacing $\boldsymbol{\mu}$ on the master side by $\boldsymbol{\mu}+\Delta\boldsymbol{\mu}$, where $\Delta\boldsymbol{\mu}$ is the sum of Dirac distributions. To overcome this conflict, we propose a modification more in the spirit of mortar techniques and use momentum free L^2-functions to define $\Delta\boldsymbol{\mu}$.

5.2.1. *Formulation.* We proceed analogously to [8], and focus on a slave element T^{s} of the surface grid $\mathcal{T}^{\mathrm{s}}$ with n_{s} denoting the numbers of its vertices. Requiring that the modified Lagrange multipliers still preserve a lowest order momentum, the modification $\Delta\boldsymbol{\mu}$ will be given in terms of

$$\Delta\phi_{pq} = \phi_p^{\mathrm{s}} d_{pp}^{-1} - \phi_q^{\mathrm{s}} d_{qq}^{-1}. \tag{33}$$

It is obvious that $\int_{T^{\mathrm{s}}} \Delta\phi_{pq}\,\mathrm{d}T^{\mathrm{s}} = 0$, thus, a lowest order momentum will be preserved. On T^{s}, any given discrete Lagrange multiplier $\boldsymbol{\mu}\in M_h$ can be written as $\boldsymbol{\mu}|_{T^{\mathrm{s}}} = \sum_{p=1}^{n_{\mathrm{s}}} \boldsymbol{\alpha}_p\mu_p$ with coefficients $\boldsymbol{\alpha}_p\in\mathbb{R}^d$, $p=1,\dots n_{\mathrm{s}}$. Its modification $\Delta\boldsymbol{\mu}$ is defined by

$$\Delta\boldsymbol{\mu}|_{T^{\mathrm{s}}} = \frac{1}{2}\sum_{p,q}\gamma_{pq}\Delta\phi_{pq}\left(\sum_{i=1}^{d}(\boldsymbol{\alpha}_p\cdot\boldsymbol{b}_p^{(i)} + \boldsymbol{\alpha}_q\cdot\boldsymbol{b}_q^{(i)})\Delta\boldsymbol{b}_{pq}^{(i)}\right), \tag{34}$$

yielding the modified multiplier $\boldsymbol{\mu}^{\mathrm{mod}} = \boldsymbol{\mu}+\Delta\boldsymbol{\mu}$. In the formula above, the coefficients γ_{pq} are the elements of a modification matrix $G\in\mathbb{R}^{n_{\mathrm{s}}\times n_{\mathrm{s}}}$ which has yet to be defined, and $\Delta\boldsymbol{b}_{pq}^{(i)} = \boldsymbol{b}_p^{(i)} - \boldsymbol{b}_q^{(i)}$, $i=1,\dots,d$.

In order to motivate our choice for the modification $\Delta\boldsymbol{\mu}$, we introduce the matrix $\boldsymbol{N}_{\mathrm{s}}\in\mathbb{R}^{d\times n_{\mathrm{s}}}$ by

$$\boldsymbol{N}_{\mathrm{s}} = (\boldsymbol{n}_1^{\mathrm{s}},\dots,\boldsymbol{n}_{n_{\mathrm{s}}}^{\mathrm{s}}),$$

where $\boldsymbol{n}_p^{\mathrm{s}}$ indicates the unit normal vector on Γ in the slave node p, $p=1,\dots,n_{\mathrm{s}}$. Moreover, the symbolic vectors Φ_{s} and Λ_{s} of length n_{s} are given by

$$\Phi_{\mathrm{s}} = (\phi_1^{\mathrm{s}},\dots,\phi_{n_{\mathrm{s}}}^{\mathrm{s}})^{\mathrm{T}},\quad \Lambda_{\mathrm{s}} = (\mu_1,\dots,\mu_{n_{\mathrm{s}}})^{\mathrm{T}},$$

where, as before, ϕ_p^{s} and μ_p denote scalar nodal basis functions of the corresponding spaces, $p=1,\dots,n_{\mathrm{s}}$. Again, we require that the modification guarantees a discrete preservation of quantities which are constant in normal and tangential direction. In contrast to the first modification, we now want to preserve these quantities when transferring between the trace space W_h^{s} and the Lagrange multiplier space M_h. This idea is motivated by the observation that $\sum_p \boldsymbol{n}_p\phi_p^s$ yields a quite good approximation of the normal field on Γ whereas $\sum_p \boldsymbol{n}_p\mu_p^s$ gives a bad result, see [8]. Because of the duality between μ_p and ϕ_q^s this does not affect the surface traction on the slave side but on the master side. In particular, focusing on the normal direction, this requirement can be expressed element-wise by demanding that $\boldsymbol{N}_{\mathrm{s}}\Lambda_{\mathrm{s}} = \boldsymbol{N}_{\mathrm{s}}\Phi_{\mathrm{s}}$. However, when usual dual basis functions are used for M_h, this cannot be achieved. But for our modification (34), we can show that

$$(\boldsymbol{N}_{\mathrm{s}}\Lambda_{\mathrm{s}})^{\mathrm{mod}} = \boldsymbol{N}_{\mathrm{s}}\Phi_{\mathrm{s}}. \tag{35}$$

Lemma 6. *Let the scalar dual basis functions be defined as in Section 4.1, namely,* $\Lambda_s = D_{T^s}M_{T^s}^{-1}\Phi_s$. *Then, the choice* $G = \frac{1}{2}D_{T^s}M_{T^s}^{-1}D_{T^s}$ *yields* (35).

Proof. From (34), we observe that

$$(\mu_p\boldsymbol{n}_p)^{\mathrm{mod}} = \mu_p\boldsymbol{n}_p + \sum_q \gamma_{pq}\Delta\phi_{pq}(\boldsymbol{n}_p - \boldsymbol{n}_q),\quad p=1,\dots,n_{\mathrm{s}},$$

which yields, using the symmetry of G, that

$$(\boldsymbol{N}_{\mathrm{s}}\Lambda_{\mathrm{s}})^{\mathrm{mod}} = \boldsymbol{N}_{\mathrm{s}}\Lambda_{\mathrm{s}} - 2\boldsymbol{N}_{\mathrm{s}}(G-D_G)D_{T^{\mathrm{s}}}^{-1}\Phi_{\mathrm{s}}$$

with a diagonal matrix D_G defined by $(D_G)_{pp} = \sum_q \gamma_{pq}$. The definitions $\Lambda_\mathrm{s} = D_{T^\mathrm{s}} M_{T^\mathrm{s}}^{-1} \Phi_\mathrm{s}$ and $G = \frac{1}{2} D_{T^\mathrm{s}} M_{T^\mathrm{s}}^{-1} D_{T^\mathrm{s}}$ imply

$$(\boldsymbol{N}_\mathrm{s}\Lambda_\mathrm{s})^\mathrm{mod} = \boldsymbol{N}_\mathrm{s}(D_{T^\mathrm{s}} M_{T^\mathrm{s}}^{-1} - 2GD_{T^\mathrm{s}}^{-1} + 2D_G D_{T^\mathrm{s}}^{-1})\Phi_\mathrm{s} = \boldsymbol{N}_\mathrm{s}(2D_G D_{T^\mathrm{s}}^{-1})\Phi_\mathrm{s}.$$

We note that the row sums of D_{T^s} and M_{T^s} are equal,

$$(D_{T^\mathrm{s}}\mathbf{1})_p = \int_{T^\mathrm{s}} \phi_p^\mathrm{s} \,\mathrm{d}T^\mathrm{s} = \sum_q \int_{T^\mathrm{s}} \phi_p^\mathrm{s}\phi_q^\mathrm{s} \,\mathrm{d}T^\mathrm{s} = (M_{T^\mathrm{s}}\mathbf{1})_p, \qquad p = 1, \dots, n_\mathrm{s},$$

yielding $D_{T^\mathrm{s}} M_{T^\mathrm{s}}^{-1} D_{T^\mathrm{s}} \mathbf{1} = D_{T^\mathrm{s}}\mathbf{1}$, from which it becomes obvious that $2D_G D_{T^\mathrm{s}}^{-1} = \mathrm{Id}$, which concludes the proof. □

5.2.2. *Analysis.* In contrast to subsection 5.1, we apply the modification in a symmetric way and work on

$$V_h^\mathrm{mod} \;=\; \left\{ \boldsymbol{v} \in X_h : \left(\boldsymbol{\mu}_p^i, \boldsymbol{v}_\mathrm{s} - (\boldsymbol{\mu}_p^i + \Delta\boldsymbol{\mu}_p^i)\boldsymbol{v}_\mathrm{m}\right)_{L^2(\Gamma_h^\mathrm{s})} = 0,\ p \in \mathcal{V}^\mathrm{s},\ i = 1, \dots d \right\}.$$

In the definition above, $\boldsymbol{\mu}_p^i = \mu_p \boldsymbol{e}_i$ denotes the vectorial basis function of the Lagrange multiplier space M_h in direction x_i associated with the slave node p, and $\Delta\boldsymbol{\mu}_p^i$ stands for its modification according to (34).

Lemma 7. *Let the modification be given by* (34)*. Then, for an arbitrary $\boldsymbol{v} = (\boldsymbol{v}_m, \boldsymbol{v}_s) \in V_h$, there exists $\Delta\boldsymbol{v} \in X_h$ such that*

$$\boldsymbol{v}^\mathrm{mod} = \boldsymbol{v} + \Delta\boldsymbol{v} \in V_h^\mathrm{mod}, \tag{36a}$$

$$\|\Delta\boldsymbol{v}\|_{X_h} \le Ch^{t+1/2} |\boldsymbol{v}_m|_{t,\Gamma_h^m}, \qquad t \in [0,1], \tag{36b}$$

$$\|\Delta\boldsymbol{v}\|_{0,\Gamma_h^s} \le Ch^{3/2} |\boldsymbol{v}_m|_{1/2,\Gamma_h^m}, \tag{36c}$$

$$\|\boldsymbol{v}\|_{X_h} \sim \|\boldsymbol{v}^\mathrm{mod}\|_{X_h}, \qquad h \text{ small enough.} \tag{36d}$$

The analogous statement holds for arbitrary $\boldsymbol{v}^\mathrm{mod} \in V_h^\mathrm{mod}$.

Proof. We proceed analogously to the proof of Lemma 3 in [8] for the two-dimensional case. Let $\Delta\boldsymbol{v} \in X_h$ be defined by

$$\Delta\boldsymbol{v} \;=\; \left(0\,,\, \sum_{p\in\mathcal{V}^\mathrm{s}} \phi_p^\mathrm{s}\boldsymbol{\beta}_p\right),\ \boldsymbol{\beta}_p \in \mathbb{R}^d \text{ with components } \beta_p^i = \frac{(\Delta\boldsymbol{\mu}_p^i,\ P_\mathrm{s}\boldsymbol{v}_\mathrm{m})_{L^2(\Gamma_h^\mathrm{s})}}{(\mu_p,\ \phi_p^\mathrm{s})_{L^2(\Gamma_h^\mathrm{s})}}. \tag{37}$$

It follows that

$$\boldsymbol{v}^\mathrm{mod} = \boldsymbol{v} + \Delta\boldsymbol{v} \in V_h^\mathrm{mod} \tag{38a}$$

$$\|\Delta\boldsymbol{v}\|_{X_h}^2 \le Ch^{d-2} \sum_{p\in\mathcal{V}^\mathrm{s}, i=1,\dots,d} (\beta_p^i)^2, \tag{38b}$$

$$\|\Delta\boldsymbol{v}\|_{0,\Gamma_h^\mathrm{s}}^2 \le Ch^{d-1} \sum_{p\in\mathcal{V}^\mathrm{s}, i=1,\dots,d} (\beta_p^i)^2. \tag{38c}$$

It remains to estimate the coefficients β_p^i. On a slave element $T^\mathrm{s} \in \mathcal{T}^\mathrm{s}$, we obtain from (34) for the Lagrange multiplier basis function $\Delta\boldsymbol{\mu}_p^i$, $i \in \{1, \dots, d\}$, associated with the node p, that

$$\Delta\boldsymbol{\mu}_p^i|_{T^\mathrm{s}} = \sum_q \gamma_{pq} \Delta\phi_{pq} \left(\sum_{k=1}^d (\boldsymbol{e}_i \cdot \boldsymbol{b}_p^{(k)}) \Delta\boldsymbol{b}_{pq}^{(k)} \right). \tag{39}$$

Due to the proper scaling of the difference $\Delta\phi_{pq}$ given by (33), we can use the piecewise constant L^2-projection onto the slave elements, indicated by Π_0, and obtain, considering the fact that the

area of the support of μ_p and ϕ_p^{s} is $O(h^{d-1})$, that

$$
\begin{aligned}
(\beta_p^i)^2 \;&=\; \left(\frac{\left(\Delta \boldsymbol{\mu}_p^i,\; P_{\mathrm{s}} \boldsymbol{v}_{\mathrm{m}} - \Pi_0 P_{\mathrm{s}} \boldsymbol{v}_{\mathrm{m}}\right)_{0,\Gamma_h^{\mathrm{s}}}}{\left(\mu_p,\; \phi_p^{\mathrm{s}}\right)_{0,\Gamma_h^{\mathrm{s}}}} \right)^2 \\
&\leq\; \frac{C}{(h^{d-1})^2} \left(\Delta \boldsymbol{\mu}_p^i,\; P_{\mathrm{s}} \boldsymbol{v}_{\mathrm{m}} - \Pi_0 P_{\mathrm{s}} \boldsymbol{v}_{\mathrm{m}}\right)_{0,\Gamma_h^{\mathrm{s}}}^2 .
\end{aligned}
$$

Setting $\Gamma_h^p = \operatorname{supp} \mu_p$, we denote by $\mathcal{T}^p \subset \mathcal{T}^{\mathrm{s}}$ the set of all slave elements T^{s} such that $\Gamma_h^p \cap T^{\mathrm{s}}$ has a positive $(d-1)$-dimensional measure, and remark that $|\mathcal{T}^p| < C$. By using the Cauchy-Schwarz inequality, it follows that, for $t \in [0,1]$,

$$
\begin{aligned}
(\beta_p^i)^2 \;&\leq\; C(h^{1-d})^2 \sum_{T^{\mathrm{s}} \in \mathcal{T}^p} \|\Delta \boldsymbol{\mu}_p^i\|_{0,T^{\mathrm{s}}}^2 \|P_{\mathrm{s}} \boldsymbol{v}_{\mathrm{m}} - \Pi_0 P_{\mathrm{s}} \boldsymbol{v}_{\mathrm{m}}\|_{0,T^{\mathrm{s}}}^2 \\
&\leq\; C(h^{t+1-d})^2 |P_{\mathrm{s}} \boldsymbol{v}_{\mathrm{m}}|_{t,\Gamma_h^p}^2 \|\Delta \boldsymbol{\mu}_p^i\|_{0,\Gamma_h^p}^2 .
\end{aligned}
$$

Considering (23), (33), and the definition of G in Lemma 6, an investigation of the terms appearing in (39) yields $\|\Delta \boldsymbol{\mu}_p^i\|_{0,\Gamma_h^p}^2 = O(h^{d+1})$, and, therefore,

$$
(\beta_p^i)^2 \;\leq\; C h^{2t+3-d} |P_{\mathrm{s}} \boldsymbol{v}_{\mathrm{m}}|_{t,\Gamma_h^p}^2 .
$$

Summing up, the stability of the projection P_{s} and (38b) imply (36b), and, choosing $t = 1/2$, (38c) yields (36c). The norm equivalence (36d) follows from (36b) and the trace theorem by observing that

$$
\|\boldsymbol{v}\|_{X_h} \begin{cases} \geq \|\boldsymbol{v}^{\mathrm{mod}}\|_{X_h} - \|\Delta \boldsymbol{v}\|_{X_h} \geq (1 - C h_{\mathrm{s}}) \|\boldsymbol{v}^{\mathrm{mod}}\|_{X_h}, \\ \leq \|\boldsymbol{v}^{\mathrm{mod}}\|_{X_h} + \|\Delta \boldsymbol{v}\|_{X_h} \leq (1 + C h_{\mathrm{s}}) \|\boldsymbol{v}^{\mathrm{mod}}\|_{X_h}, \end{cases}
$$

provided that h_{s} is small enough. According to (37), we observe that $\Delta \boldsymbol{v}$ only depends on $\boldsymbol{v}_{\mathrm{m}} = \boldsymbol{v}_{\mathrm{m}}^{\mathrm{mod}}$. Therefore, it is obvious that the analogous statement of the Lemma has to hold for an arbitrary $\boldsymbol{v}^{\mathrm{mod}} \in V_h^{\mathrm{mod}}$. □

The main difference between Lemma 3 and Lemma 7 is that we can exploit the fact that $\Delta \boldsymbol{\mu}$ is orthogonal on a constant with respect to the L^2-scalar product. Thus the upper bounds (36b) and (36c) provide a higher order than the bounds (28b) and (28c), respectively.

By using Lemma 7, the proof of the V_h^{mod}-ellipticity is completely analogous to the proof of Lemma 4, the estimation of the consistency error follows the lines of Lemma 5. However, from Lemma 7, it can be seen that the modification only enters in terms of $O(h^{3/2})$. It remains to prove the approximation property of V_h^{mod}. For convenience, we repeat the statement and the proof given in [8].

Lemma 8. *It holds that*

$$
\inf_{\boldsymbol{v}_h^{\mathrm{mod}} \in V_h^{\mathrm{mod}}} \|\boldsymbol{u} - \boldsymbol{v}_h^{\mathrm{mod}}\|_{X_h} \;\leq\; C h \|\boldsymbol{u}\|_{2,\Omega}. \tag{40}
$$

Proof. From the unmodified approach, we can find $\boldsymbol{v}_h \in V_h$ such that

$$
\|\boldsymbol{u} - \boldsymbol{v}_h\|_{X_h} \leq C h \|\boldsymbol{u}\|_{2,\Omega}.
$$

We choose $\boldsymbol{v}_h^{\mathrm{mod}} \in V_h^{\mathrm{mod}}$ as in Lemma 7, and obtain

$$
\begin{aligned}
\|\boldsymbol{u} - \boldsymbol{v}_h^{\mathrm{mod}}\|_{X_h}^2 \;&\leq\; C \|\boldsymbol{u} - \boldsymbol{v}_h\|_{X_h}^2 + C \|\Delta \boldsymbol{v}_h\|_{X_h}^2 \leq C h^2 \|\boldsymbol{u}\|_{2,\Omega}^2 + C h^3 |\boldsymbol{v}_m|_{1,\Gamma_h^m}^2 \\
&\leq\; C h^2 (1 + h) \|\boldsymbol{u}\|_{2,\Omega}^2 .
\end{aligned} \tag{41}
$$

We observe again that the modification only enters with $O(h^{3/2})$. □

5.3. **Numerical results.** In order to present the effect of our modifications, we investigate a 3D example which is analogous to the 2D example given in [8]. The global domain is a spherical shell with inner radius $r_i = 0.9$ and outer radius $r_o = 1.1$, its material data given by $E = 1.0$ and $\nu = 0.3$. The outer boundary $\{\boldsymbol{x} \in \mathbb{R}^3 : |\boldsymbol{x}| = 1.1\}$ is fixed by enforcing homogeneous Dirichlet boundary conditions, whereas on the inner boundary $\{\boldsymbol{x} \in \mathbb{R}^3 : |\boldsymbol{x}| = 0.9\}$, a uniform radial pressure of magnitude -1 is applied. The symmetry of the domain and the problem data yields the exact solution $u(r) = a/r^2 + br$, depending only on $r(\boldsymbol{x}) = |\boldsymbol{x}|$, with $b = 1/(3\lambda + 2\mu + 4\mu r_o^3/r_i^3)$ and $a = -br_o^3$. In order to keep a full 3D setting, we exploit the radial symmetry only partially for the numerical simulation of the problem, namely, by considering only the octant $O_1 = \{\boldsymbol{x} \in \mathbb{R}^3 : x_i > 0,\ i = 1, 2, 3\}$. The interface Γ is set to be the unit sphere intersected by O_1, yielding the subdomains $\Omega^{\mathrm{m}} = \{\boldsymbol{x} \in O_1 : |\boldsymbol{x}| \in (r_i, 1)\}$ and $\Omega^{\mathrm{s}} = \{\boldsymbol{x} \in O_1 : |\boldsymbol{x}| \in (1, r_o)\}$. The additional boundary conditions on the symmetry boundaries $\Sigma_i = (\overline{\Omega^{\mathrm{m}} \cup \Omega^{\mathrm{s}}}) \cap \{\boldsymbol{x} \in \mathbb{R}^3 : x_i = 0\}$, $i = 1, \ldots, 3$, are given by $\boldsymbol{u} \cdot \boldsymbol{n}_i = 0$ and $\sigma_t = 0$, where $\boldsymbol{n}_i = -\boldsymbol{e}_i$ is the corresponding normal vector and σ_t indicates the tangential part of the surface traction $\sigma(\boldsymbol{u})\boldsymbol{n}_i$. For a detailed account on how to handle the Lagrange multiplier nodes on $\Sigma_i \cap \overline{\Gamma}$, we refer to [9].

Visible undesired oscillations occur only when the surface grid $\mathcal{T}^{\mathrm{s}}$ on the slave side is considerably coarser than the grid $\mathcal{T}^{\mathrm{m}}$ on the master side. To this end, we first take a ratio of $h_{\mathrm{s}}/h_{\mathrm{m}} = 4/1$, and the corresponding surface grids consist of 12 and 192 elements for $\mathcal{T}^{\mathrm{s}}$ and $\mathcal{T}^{\mathrm{m}}$, respectively. In radial direction, we take two elements for each subdomain, giving a total of 408 volume elements. In Figure 3, the deformed domain is visualized for four different approaches: the unmodified dual

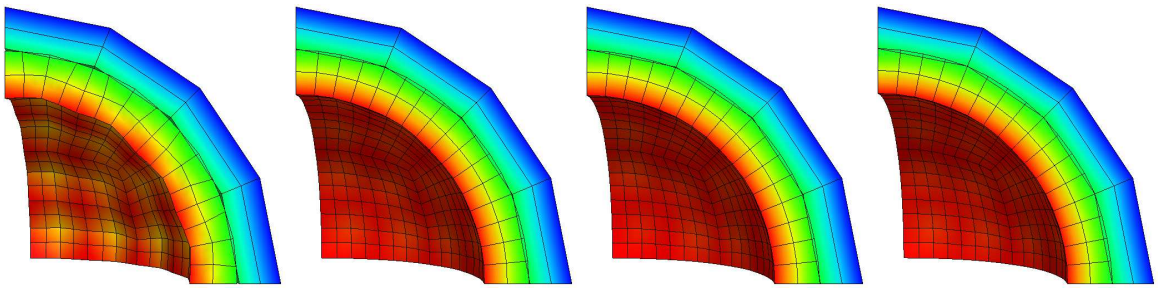

FIGURE 3. Ratio $h_{\mathrm{s}}/h_{\mathrm{m}} = 4/1$, distorted domains: unmodified dual (left), modifications 1 and 2 (middle), and standard Lagrange multipliers (right).

one, the modified ones as introduced in Sections 5.1 and 5.2, and, as a reference, the one taking standard basis functions. The solution of the unmodified dual method is subject to oscillations. The two modifications give equally good results, the surface tractions and the displacements, which are both constant in normal direction, are interchanged between the grids in the expected correct way. We increase the ratio $h_{\mathrm{s}}/h_{\mathrm{m}}$ further to 8/1, taking 768 elements for $\mathcal{T}^{\mathrm{m}}$, and four elements in radial direction, giving 3120 volume elements. The corresponding deformed domains are visualized in Figure 4. For the unmodified dual approach, the oscillations become worse, while

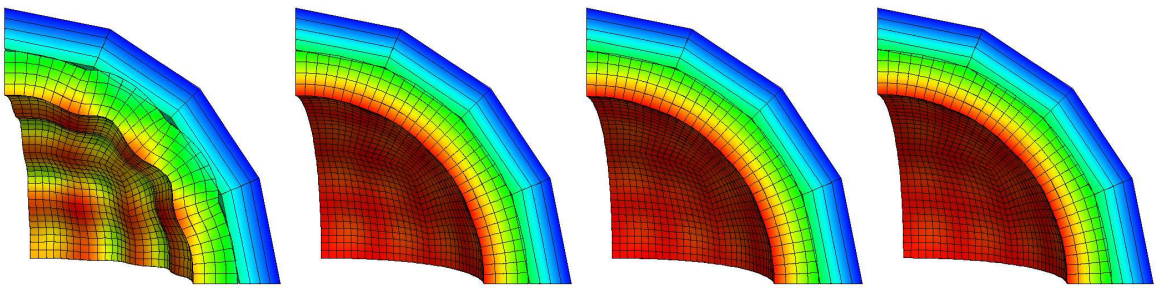

FIGURE 4. Ratio $h_{\mathrm{s}}/h_{\mathrm{m}} = 8/1$, distorted domains: unmodified dual (left), modifications 1 and 2 (middle), and standard Lagrange multipliers (right).

the other three considered methods remain stable. We emphasize that the effect only occurs when the Lagrange multipliers are chosen with respect to the coarse side. Thus, in this simple example, one could avoid any complications by choosing the multipliers on the finer grid. However, in more general settings, the ratio h_{T^s}/h_{T^m} for two intersecting elements from the master and slave side can vary drastically over the global interface Γ. Moreover, the choice of the grid for the Lagrange multipliers may be dictated by the problem formulation. Our modifications introduced in Sections 5.1 and 5.2 admit the possibility to stay flexible and still keep all the advantages of the dual approach.

6. An application to a nonlinear elasticity problem

As an example for a nonlinear elasticity problem, we consider a global domain consisting of three hexahedrons $\Omega^{m,1}$, $\Omega^{m,2}$, and Ω^s. The two master subdomains $\Omega^{m,1}$ and $\Omega^{m,2}$ are cubes of edge length 2. The slave subdomain Ω^s, a cuboid of base area 4 and variable height H, is placed between the two master subdomains. While Poisson's ratio $\nu = 0.3$ is constant on all subdomains, Young's modulus E is set to be 10^5 on $\Omega^{m,1}$, $\Omega^{m,2}$, and 10^2 on Ω^s. The lowest subdomain $\Omega^{m,1}$ is fixed at its lower face, while on the upper face of the upper subdomain $\Omega^{m,2}$, a rotation of $\pi/8$ parallel to the (x, y)-plane is applied. The material parameters suggest to use a finer grid on the slave subdomain Ω^s, which is easily possible by using non-matching grids. Moreover, on each subdomain, individual elasticity model equations can be considered: linearized (7)-(9), geometrically nonlinear (10)-(12), and Neo-Hooke (12)-(13).

Figure 5 shows the deformed domain, once using the linear model on all subdomains, and once using the Neo-Hooke law everywhere. As was to be expected, the linearized equations do not give

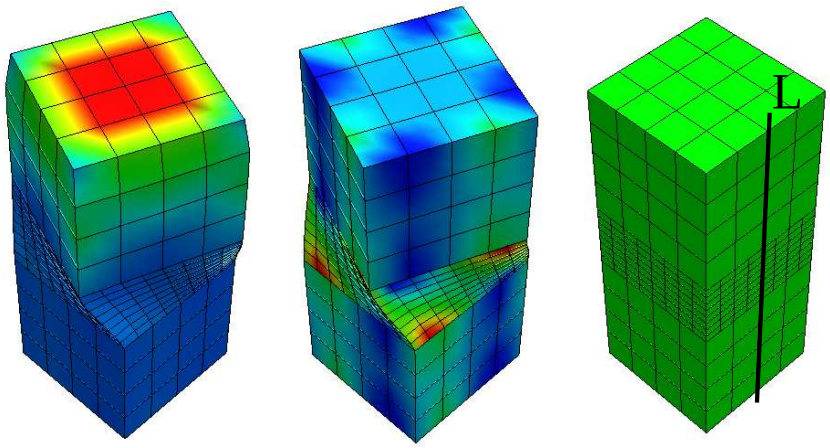

Figure 5. Deformed domains for the linearized (left) and the Neo-Hooke setting (middle). The line L (right).

a visually satisfying result for the upper cube $\Omega^{m,2}$. There the displacement is almost a pure, but large rotation, which cannot be modeled correctly by (7)-(9). Visually, the method using the Neo-Hooke law everywhere yields correct results. However, the problem setting and the solution suggest that it might not be necessary to use the fully nonlinear and complicated Neo-Hooke model on all three subdomains. On the upper cube $\Omega^{m,2}$, it should be enough to consider the geometrically nonlinear setting, because large deformations, but relatively small strains occur. On the lower cube $\Omega^{m,1}$, also the deformations remain small, and the linearized model might be sufficient. On the middle subdomain Ω^s, both the deformations and the strains are quite large, there, the Neo-Hooke law should be mandatory. In Figure 6, the displacements in x-, y-, and z-direction are plotted along the line L, which is indicated in the right picture of Figure 5. The notation ijk, $i, j, k = l, g, n$, indicates that models i, j, and k are used on $\Omega^{m,2}$, Ω^s, and $\Omega^{m,1}$, respectively. As was already suggested by the domain deformations in Figure 5, the fully linear

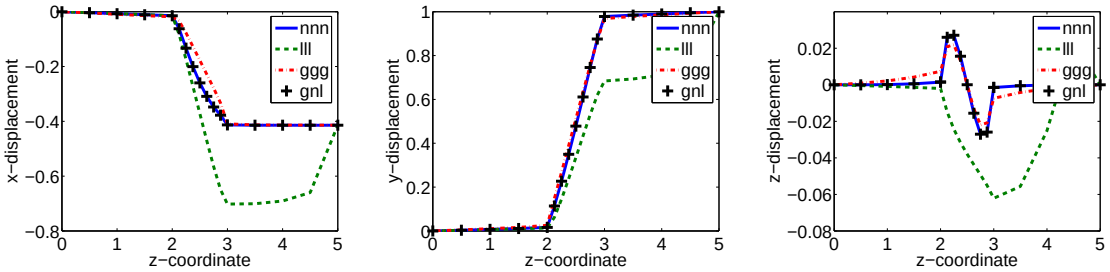

FIGURE 6. Different model equations: displacements in x-, y-, and z-direction along the line L.

model *lll* fails completely. Also, the geometrically nonlinear setting *ggg* cannot resolve all features of the reference solution *nnn* which uses the Neo-Hooke law everywhere. However, the combination *gnl*, as discussed above, gives results which cannot be distinguished from the reference solution.

In our next test, the thickness H of the slave subdomain is varied. In Figure 7, the deformed domains are plotted for $H = 1, 0.5, 0.25, 0.125$, using the Neo-Hooke law on all subdomains. Analogously to Figure 6, the displacements along the line L are given in Figure 8.

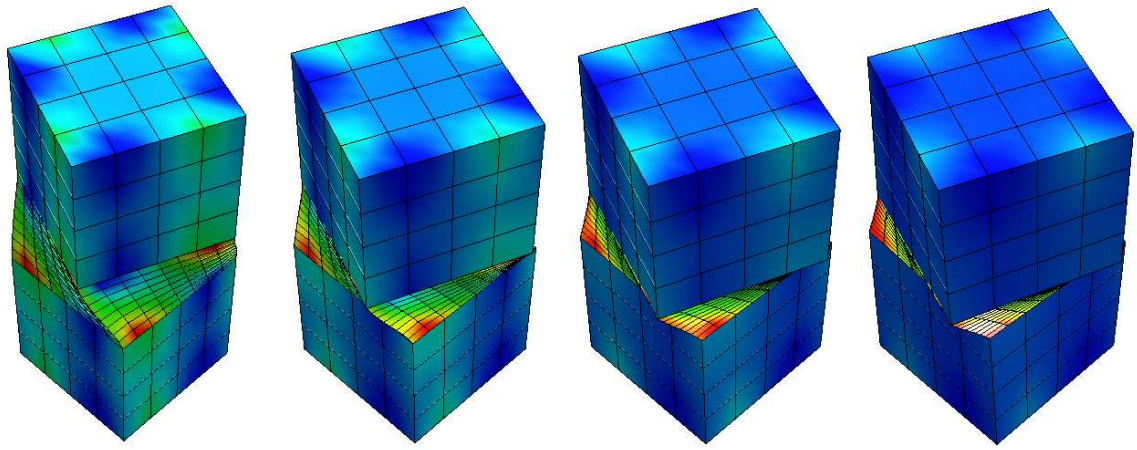

FIGURE 7. Variation of H: 1, 0.5, 0.25, 0.125.

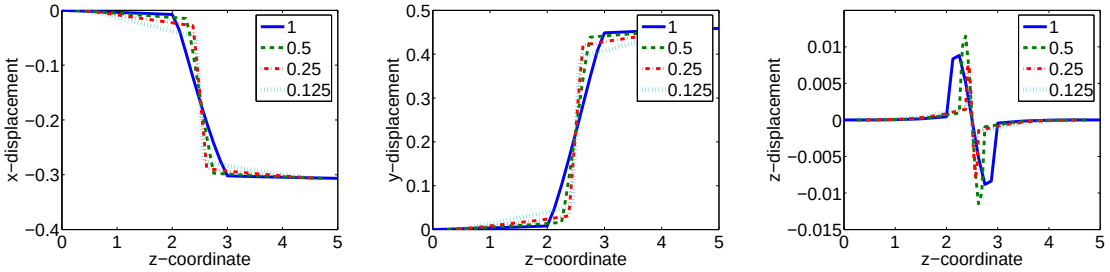

FIGURE 8. Variation of H: displacements in x-, y-, and z-direction along the line L.

REFERENCES

[1] D. N. Arnold, D. Boffi, and R. S. Falk. Approximation by quadrilateral finite elements. *Math. Comp.*, 71(239):909–922, 2002.

[2] F. Ben Belgacem. The mortar finite element method with Lagrange multipliers. *Numer. Math.*, 84(2):173–197, 1999.
[3] C. Bernardi, Y. Maday, and A. T. Patera. A new nonconforming approach to domain decomposition: the mortar element method. In *Nonlinear partial differential equations and their applications. Collège de France Seminar, Vol. XI (Paris, 1989–1991)*, volume 299 of *Pitman Res. Notes Math. Ser.*, pages 13–51. Longman Sci. Tech., Harlow, 1994.
[4] D. Braess and W. Dahmen. Stability estimates of the mortar finite element method for 3-dimensional problems. *East-West J. Numer. Math.*, 6(4):249–263, 1998.
[5] F. Brezzi and D. Marini. Error estimates for the three-field formulation with bubble stabilization. *Math. Comp*, 70:911–934, 2001.
[6] A. Ern and J.-L. Guermond. *Theory and practice of finite elements*, volume 159 of *Applied Mathematical Sciences*. Springer-Verlag, New York, 2004.
[7] B. Flemisch, J. Melenk, and B. I. Wohlmuth. Mortar methods with curved interfaces. *Appl. Numer. Math.*, 54(3-4):339–361, 2005.
[8] B. Flemisch, M. A. Puso, and B. I. Wohlmuth. A new dual mortar method for curved interfaces: 2D elasticity. *Internat. J. Numer. Methods Engrg.*, 63(6):813–832, 2005.
[9] B. Flemisch and B. I. Wohlmuth. Nonconforming methods for nonlinear elasticity problems. Technical Report 03, Universität Stuttgart, SFB 404, 2005.
[10] J. Gopalakrishnan. *On the mortar finite element method*. PhD thesis, Texas A&M University, 1999.
[11] P. Hauret. *Numerical methods for the dynamic analysis of twoscale incompressible nonlinear structures*. PhD thesis, Ecole Polytechnique, Paris, 2004.
[12] P. Hauret and P. L. Tallec. Stabilized discontinuous mortar formulation for elastostatics and elastodynamics problems - Part I: formulation and analysis. *CMAP Internal Report 553*, 2004.
[13] P. Hauret and P. L. Tallec. A stabilized discontinuous mortar formulation for elastostatics and elastodynamics problems - Part II: discontinuous Lagrange multipliers. *CMAP Internal Report 554*, 2004.
[14] S. Hüeber and B. I. Wohlmuth. A primal-dual active set strategy for non–linear multibody contact problems. *Comput. Methods Appl. Mech. Engrg.*, 194:3147–3166, 2005.
[15] C. Kim, R. D. Lazarov, J. E. Pasciak, and P. S. Vassilevski. Multiplier spaces for the mortar finite element method in three dimensions. *SIAM J. Numer. Anal.*, 39(2):519–538, 2001.
[16] P. Seshaiyer and M. Suri. *hp* submeshing via non-conforming finite element methods. *Comput. Methods Appl. Mech. Engrg.*, 189(3):1011–1030, 2000.
[17] B. I. Wohlmuth. A mortar finite element method using dual spaces for the Lagrange multiplier. *SIAM J. Numer. Anal.*, 38(3):989–1012 (electronic), 2000.
[18] B. I. Wohlmuth. A $\mathcal{V}$-cycle multigrid approach for mortar finite elements. *SIAM J. Numer. Anal.*, 42(6):2476–2495, 2004.

Bernd Flemisch
Institut für Angewandte Analysis und Numerische Simulation
Pfaffenwaldring 57
70569 Stuttgart
Germany
E-Mail: flemisch@ians.uni-stuttgart.de
WWW: http://www.ians.uni-stuttgart.de/nmh/flemisch/flemisch.shtml

Barbara Wohlmuth
Institut für Angewandte Analysis und Numerische Simulation
Pfaffenwaldring 57
70569 Stuttgart
Germany
E-Mail: wohlmuth@ians.uni-stuttgart.de
WWW: http://www.ians.uni-stuttgart.de/nmh/wohlmuth/wohlmuth.shtml

Erschienene Preprints ab Nummer 2005/001

Komplette Liste: `http://preprints.ians.uni-stuttgart.de`

2005/001 *S. Nicaise, A.-M. Sändig*: Dynamical crack propagation in a 2D elastic body. The out-of plane state.

2005/002 *S. Hüeber, A. Matei, B.I. Wohlmuth*: A mixed variational formulation and an optimal a priori error estimate for a frictional contact problem in elasto-piezoelectricity

2005/003 *A.-M. Sändig*: Distributionentheorie mit Anwendungen auf partielle Differentialgleichungen. Vorlesung im Wintersemester 2004/2005

2005/004 *A.-M. Sändig, T. Buchukuri, O. Chkadua, D. Natroshvili*: Solvability and regularity results to boundary-transmission problems for metallic and piezoelectric elastic materials

2005/005 *B. Flemisch, B. I. Wohlmuth*: Stable Lagrange multipliers for quadrilateral meshes of curved interfaces in 3D